

Portland State University

PDXScholar

Electrical and Computer Engineering Faculty
Publications and Presentations

Electrical and Computer Engineering

6-1-1989

Theory of a synchronously pumped mode-locked dye laser in the short pump pulse limit

Duncan Leo MacFarlane

Lee W. Casperson

Portland State University

Follow this and additional works at: https://pdxscholar.library.pdx.edu/ece_fac



Part of the [Electrical and Computer Engineering Commons](#)

Let us know how access to this document benefits you.

Citation Details

D. L. MacFarlane and Lee W. Casperson, "Theory of a synchronously pumped mode-locked dye laser in the short pump pulse limit," J. Opt. Soc. Am. B 6, 1175-1181 (1989).

This Article is brought to you for free and open access. It has been accepted for inclusion in Electrical and Computer Engineering Faculty Publications and Presentations by an authorized administrator of PDXScholar. Please contact us if we can make this document more accessible: pdxscholar@pdx.edu.

Theory of a synchronously pumped mode-locked dye laser in the short pump pulse limit

D. L. MacFarlane and Lee W. Casperson

Department of Electrical Engineering, Portland State University, Portland, Oregon 97207

Received December 2, 1988; accepted February 22, 1989

We study the operation of a synchronously pumped mode-locked dye laser when the pump pulse is taken as a Dirac delta function, a limit that is sometimes experimentally reasonable. We find that in this limit the model simplifies considerably and that with further assumptions the physical interpretation of synchronously pumped mode-locked operation becomes apparent. Specifically, our nonlinear dynamical model reduces to the same set of equations that govern a prepumped Q -switched laser, and from this simple picture we are able to derive approximate analytic formulas for the synchronously pumped mode-locked laser pulse width and peak intensity. Additionally, we present a closed-form solution for the output pulse in the limit of zero-cavity-length mismatch between the pump laser and the dye laser.

1. INTRODUCTION

A recent analysis of pump pulse effects in synchronously pumped mode-locked (SPML) dye lasers¹ has revealed that several of the most advanced SPML dye lasers^{2,3} operate in the regime where the character of the output pulse is unresponsive to any further shortening of the pump pulse. Experimentally, this situation occurs when the pump pulse of a SPML Rhodamine dye-laser system is shorter than a few picoseconds, a limit that was recently achieved with fiber/grating-compressed, frequency-doubled Nd:YAG lasers.^{2,3} This study would also apply to SPML dye-laser-pumped SPML dye lasers.⁴ Physically, once the pump is shorter than the rise time of the output pulse, further shortening of the pump has no effect on the output. Mathematically, this situation corresponds to a Dirac delta-function pump and therefore leads to a great simplification of the underlying model. In effect, the forced system becomes unforced, and the SPML dye laser becomes prepumped every cavity round trip.

In this paper we reduce a detailed, proven, nonlinear dynamical model^{1,5} to a point where analytic exploration becomes possible, while the character of SPML operation is retained. In particular, we consider two limits, both of which predict pulses that are in qualitative agreement with the full model that agrees quantitatively with experiment. The first limit considered is the rate-equation approximation, and here we find a parallel between SPML systems and giant-pulsed, or Q -switched, lasers.⁶⁻⁹ That gain switching should follow as an extreme form of gain modulation seems reasonable—even intuitive; however, the traditional Q -switching model neglects semiclassical effects, which we find to be equally important to pulse development on the time scales considered here. Our second limit is one of zero-length mismatch between the pump laser and the SPML laser and mathematically corresponds to what is sometimes called the bad-cavity limit. The resulting set of coherent equations is somewhat simpler than the rate equations but also yields short pulse solutions, and these solutions may be

expressed analytically. Any further simplification of either of these limits causes the pulsed behavior to disappear.

In Section 2 we review the model derived in Ref. 5 and studied in Ref. 1. We consider the delta-function pump pulse limit and several other simplifying assumptions. The rate-equation limit is presented in Section 3, and parallels to Q -switched operation are discussed. In particular, we apply the approximate analytic solutions for Q -switched laser pulses developed in Ref. 10 to SPML dye-laser operation. We also derive approximate analytic formulas for the peak intensity and the pulse width. Section 4 considers the zero-detuning limit and demonstrates the importance of coherence effects in SPML operation in the short pump pulse limit. In our conclusion we use our findings to comment on the character of SPML operation and the practical significance of an ultrashort pump pulse.

2. REVIEW AND INITIAL SIMPLIFICATIONS OF THE MODEL

Our starting point is the semiclassical dye-laser amplifier model developed in Ref. 5 and studied in Ref. 1. Beginning with the density matrix equations and Maxwell's equations, Ref. 5 developed a set of ordinary, nonlinear differential equations that govern the interplay of the electric field with the molecular populations and the polarization. When the electric field is normalized to its steady-state gain saturating value, this set of equations may be written as

$$\begin{aligned} dD/dt = & -(1/\tau_2)[(1 + \tau_2/2\tau_1)D + (1 - \tau_2/2\tau_1)M \\ & + 2QA_x - Px^2], \end{aligned} \quad (1)$$

$$dM/dt = -(1/\tau_2)[-(\tau_2/2\tau_1)D + (\tau_2/2\tau_1)M - Px^2], \quad (2)$$

$$dQ/dt = -(1/T_s)(Q - ADx), \quad (3)$$

$$dA/dt = -(L/2t_c\Delta L)\left(A - \int_0^1 Qx dx\right). \quad (4)$$

In Eqs. (1)–(4), D is a normalized population difference, M is a normalized population sum, Q is a normalized polarization, and A is a normalized electric field. The dye decay time from the S_1 band to the S_0 band is τ_2 , and τ_1 is the lower manifold intraband vibrational relaxation time. T_s is the semiclassical coherence time.

A convenient benchmark system is the Rhodamine 6G laser. The fluorescence decay time of Rhodamine 6G is well known, and, as in other treatments, a value of $\tau_2 = 5 \times 10^{-9}$ sec is employed here.⁵ The vibrational relaxation time is much shorter and is not precisely known. Some studies have indicated that the vibrational relaxation times of both the upper and the lower electronic states of Rhodamine 6G are $(3 \pm 2) \times 10^{-12}$ sec.^{11,12} Other research has shown that the vibrational relaxation time may be somewhat shorter (at least in the upper electronic state, S_1), and a relaxation time of $(0.8 \pm 0.2) \times 10^{-12}$ sec has been deduced.¹³ For the present study the value of $\tau_1 = 1 \times 10^{-12}$ sec has been used.⁵ The coherence time, T_s , for Rhodamine 6G is shorter still, and its value is even more tenuous. The coherence times for several dyes, including Rhodamine 6G, have all been found to lie in the range of 0.02×10^{-12} to 2×10^{-12} sec, depending on solvents, spectral positions, and sample deterioration.¹⁴ A lower bound on the coherence time for Rhodamine 6G can be obtained from measurements of the time-resolved fluorescence spectrum, and such measurements have shown that, immediately after a short pump pulse, the fluorescence is a Lorentzian function having a full width at half-maximum of 12 nm.¹⁵ With pure homogeneous broadening, this would correspond to a homogeneous bandwidth of $\Delta\nu_h = 1.15 \times 10^{13}$ Hz and a minimum coherence time of 28×10^{-15} sec. Recent femtosecond dephasing studies have measured this coherence time for similar dyes to be less than 20×10^{-15} sec.¹⁶ Given the limitations of the available data, it was decided here simply to adopt the previously inferred value of $T_s = 50 \times 10^{-15}$ sec.^{17,18}

The dynamical rate constant associated with the field is composed of the cavity length, L , the cavity lifetime, t_c , and the optical length mismatch, ΔL , which is the amount by which the dye-laser cavity length exceeds that of the pump laser. Typically, $L = 1.8$ m, $t_c = 10$ nsec, and ΔL is small, approximately 0–30 μ m. For the shortest output pulses, ΔL is a key experimental adjustment. With regard to ultrashort pulse production, the key time constants in this set of equations are the coherence, or dephasing, time, T_s , and the cavity lifetime mismatch, $2t_c\Delta L/L$. These two time constants control the bandwidth. This model is also general enough to include explicitly the orientation of the molecular dipoles, $x = \cos \theta$. Thus, in general, Eqs. (1)–(3) refer specifically to only one orientational class, and the individual classes contribute to the field through the integral over x in Eq. (4).

$P(t)$ is the normalized pump function, and its effects were explored in detail in Ref. 1 for the Gaussian shape:

$$P(t) = P_0(2/\Delta\tau)(\ln 2/\pi)^{1/2} \exp[-(2t/\Delta\tau)^2 \ln 2]. \quad (5)$$

In Eq. (5) $\Delta\tau$ is the full width at half-maximum (FWHM) pulse width and P_0 is a measure of the pump level, which in most practical cases is directly proportional to the threshold parameter, r . The details of the ultrashort pulse production rely significantly on the gain dynamics resulting from the pump—specifically the pump integral—and these issues have been well studied.^{5,19} In general, the leading edge of

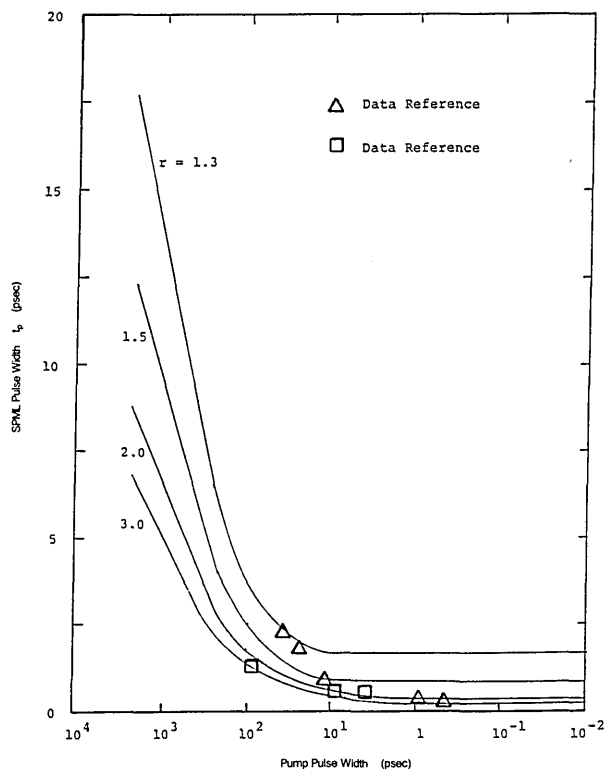


Fig. 1. SPML output pulse width, t_p , versus pump pulse width, $\Delta\tau$, at a cavity detuning of 10 μ m and for threshold parameters $r = 1.3, 1.5, 2.0, 3.0$. Superimposed upon this plot are data points taken from the literature. The triangles represent data taken from Ref. 2. The rectangles on the graph denote data from Ref. 3.

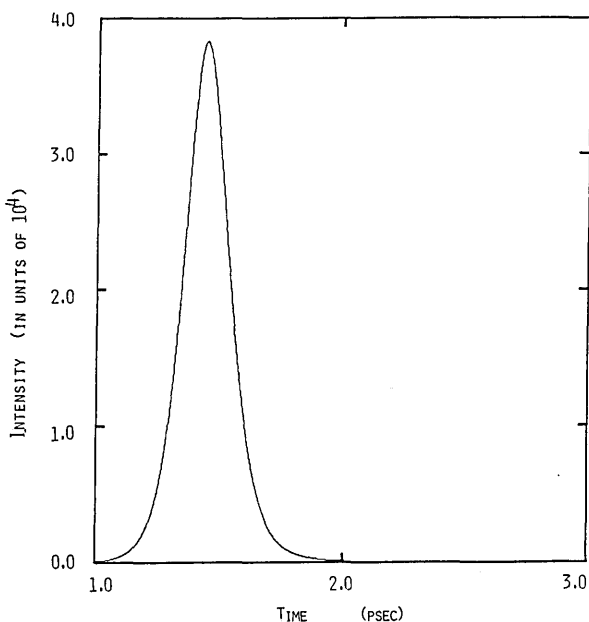


Fig. 2. Typical SPML pulse numerically calculated from Eqs. (1)–(5) for $\Delta L = 10 \mu$ m, $r = 3$, and $\Delta\tau = 100$ fsec. The FWHM output pulse width is approximately 200 fsec.

the SPML pulse is controlled largely by the unsaturated gain, while the depleted (saturated) gain is responsible for the shaping of the pulse tail. The play of coherence effects modifies this process to some extent, and thus it is important in quantitative studies to include a finite coherence time, T_s .

Of specific interest in Ref. 1 was the change in the SPML output pulse as the pump pulse width was decreased. Figure 1 shows the decrease in the output pulse width as $\Delta\tau$ is shortened through several orders of magnitude. As with all aspects of the SPML output pulse character, there is no change in the SPML pulse width as $\Delta\tau$ is shortened beyond a few picoseconds. This point is central to this paper because it shows that for $\Delta\tau \leq 1$ psec, $P(t)$ may be replaced with a Dirac delta function, $P(t) = P_0\delta(t)$. A typical pulse predicted by the set of Eqs. (1)–(5) in the delta-function limit is shown in Fig. 2. In the remainder of this section we simplify the set of Eqs. (1)–(5) by using various approximations in order to study the nature of SPML dye lasers in the delta-function limit.

One of the biggest complications to Eqs. (1)–(4) is the dipole orientation integral in the field equation. While orientational effects have been shown to be of importance in quantitative modeling of the output pulse shape, dipole orientation is not essential to the general nature of SPML operation.⁵ More formally, one might argue that with parallel pump and signal polarizations and slow rotational relaxation, only one orientational class of dye molecule would contribute to the field. Hence we consider here a unidirectional orientational distribution^{5,20} whereby the set of Eqs. (1)–(5) reduces to

$$\frac{dD}{dt} = -(1/\tau_2)[(1 + \tau_2/2\tau_1)D + (1 - \tau_2/2\tau_1)M + 2QA - P_0\delta(t)], \quad (6)$$

$$\frac{dM}{dt} = -(1/\tau_2)[-(\tau_2/2\tau_1)D + (\tau_2/2\tau_1)M - P_0\delta(t)], \quad (7)$$

$$\frac{dQ}{dt} = -(1/T_s)(Q - AD), \quad (8)$$

$$\frac{dA}{dt} = -(L/2t_c\Delta L)(A - Q). \quad (9)$$

In Eqs. (6)–(9) we have also written the pump function explicitly as a delta function.

For values of τ_1 and τ_2 relevant to typical dye lasers, we note that $\tau_2/2\tau_1 \gg 1$, and, to good approximation, Eq. (6) may be rewritten as

$$\frac{dD}{dt} = -(1/\tau_2)[(\tau_2/2\tau_1)D - (\tau_2/2\tau_1)M + 2QA - P_0\delta(t)]. \quad (10)$$

Considering the femtosecond output pulses found to be produced by this system in the delta-function pumping limit, it seems reasonable to neglect the nonradiative relaxation from the lower laser state. This limit of τ_1 long compared with the lasing action allows us to combine Eqs. (7) and (10) and to eliminate the population sum, M , and its dynamical equation. The population difference equation then becomes

$$\frac{dD}{dt} = -(1/\tau_2)[2QA - P_0\delta(t)]. \quad (11)$$

The delta function in Eq. (11) is nonzero only at $t = 0$ and therefore serves to set the initial conditions appropriate to the pumping level. At $t = 0$, $A \approx 0$, and Eq. (11) is decoupled from Eqs. (8) and (9). We integrate from $t = 0^-$ to $t = 0^+$, through the delta function, to establish the initial condition for D at a time 0^+ . Thus, immediately after the pump function, $D(0^+) = P_0/\tau_2 = r$, the threshold parameter. The corresponding initial condition for the field should be a value that represents an approximate level of spontaneous

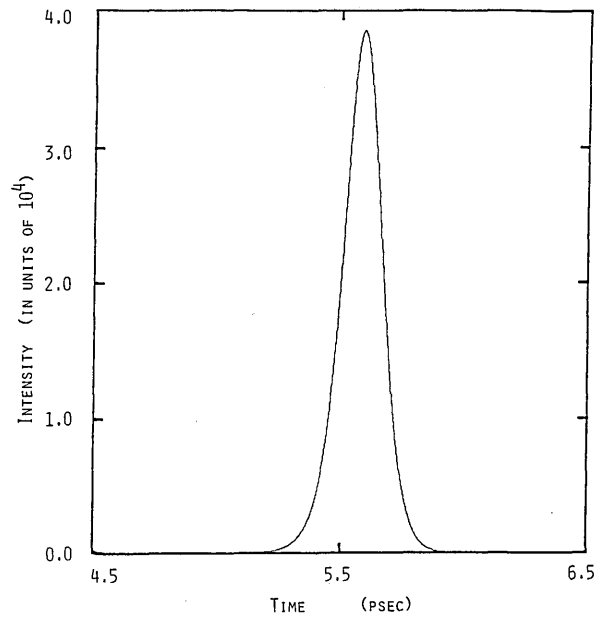


Fig. 3. Typical SPML pulse numerically calculated from Eqs. (12)–(14) for $\Delta L = 10 \mu\text{m}$ and $r = 3$.

emission. For our work, this A_0 is chosen to be 10^{-10} . For all times greater than 0, then, our set of equations is

$$\frac{dD}{dt} = -(1/\tau_2)(2AQ), \quad (12)$$

$$\frac{dQ}{dt} = -(1/T_s)(Q - AD), \quad (13)$$

$$\frac{dA}{dt} = -(L/2t_c\Delta L)(A - Q). \quad (14)$$

The output pulse predicted by this set of equations is shown in Fig. 3. Neglecting orientational effects and simplifying the energy-level scheme causes the output pulse to form 4 psec later. Notably, the peak intensity is essentially unchanged with these approximations, and there is only a slight shortening in the pulse width. We also note that Eqs. (12)–(14) correspond to the much considered Lorenz equations^{21–23} for the case of zero forcing.

In Sections 3 and 4 we consider Eqs. (12)–(14) in two limits: the rate-equation limit, $T_s = 0$, and the zero-detuning limit, $\Delta L = 0$. Interestingly, both limits yield pulses that are at least qualitatively similar to those predicted by the initial set, Eqs. (1)–(5).

3. RATE-EQUATION LIMIT

In the rate-equation approximation one ignores coherence effects and therefore the dependence of the polarization on past values of the electric field. Since a finite coherence time represents a temporal lag between the electric field and the polarization, coherence effects play an important role in limiting the magnitude and the width of short optical pulses.^{1,5,24} However, the error involved in the rate-equation limit is typically less than a factor of 2 for these systems,^{1,5} and thus, for a qualitative study, the rate-equation approximation is often reasonable. Mathematically, the rate-equation approximation is the limit of $T_s = 0$. From Eq. (13), then, $Q = AD$, and our set may be written in terms of the normalized population difference, D , and the intensity, $I \equiv A^2$:

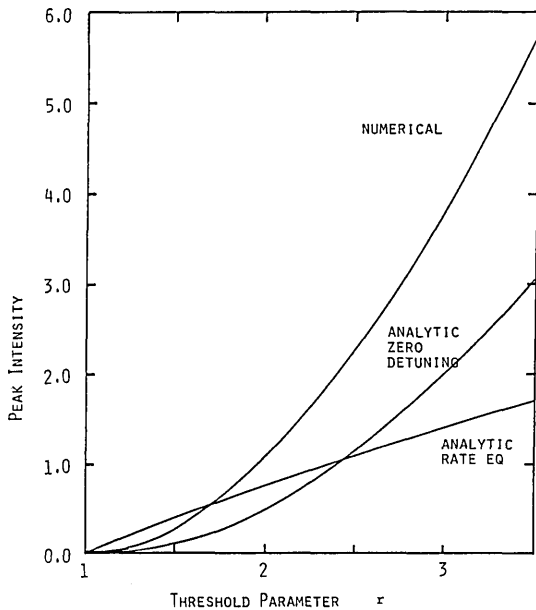


Fig. 4. Peak intensity dependence on the threshold parameter, r , calculated using Eqs. (17) and (30) and the set Eqs. (1)–(5) for typical dye-laser values. There is qualitative agreement between the approximate analytic formula for the zero-detuning limit and the more exact numerical treatment. The intensity scale is in units of 10^4 for the numerical and the rate-equation curves, but it is in units of 10^5 for the zero-detuning curve.

$$dD/dt = -(1/\tau_2)(2ID), \quad (15)$$

$$dI/dt = -(L/t_c \Delta L)(I - ID). \quad (16)$$

Equations (15) and (16) are exactly the form of the equations that describe giant pulses from Q -switched lasers,^{7–9} and it is useful to reinterpret the results of these earlier studies in the context of mode-locked lasers. This analogy between SPML dye lasers and gain-switched lasers was noted previously by Catherall *et al.*²⁵ and by Yasa.¹⁹

Dividing Eq. (15) by Eq. (16) and integrating yields the intensity as a function of D . Noting from Eq. (16) that the peak intensity occurs at $D = 1$, we may recast the familiar

formula for the peak intensity of a Q -switched laser pulse in terms of SPML laser parameters:

$$I_{pk} = (\tau_2 L / 2t_c \Delta L) [r - \ln r - 1 + 2t_c \Delta L I_0 / \tau_2 L]. \quad (17)$$

Figure 4 includes a plot of Eq. (17) as a function of r and compares it with the peak intensity calculated by Eqs. (1)–(5). We see that over the range of interest the agreement is of the correct order of magnitude.

We know of no complete analytic solution to the set of Eqs. (15) and (16). A typical approach in analytic studies involves fitting the numerical solution of Eqs. (15) and (16) to a family of analytic pulse shapes.¹⁰ Before considering specific examples of such pulses and their autocorrelations, we will study Eqs. (15) and (16) in two limits that yield, respectively, the leading edge and the falling edge of the pulse. These limits will suggest an appropriate pulse form and will allow us to estimate the mode-locked pulse width analytically.

The leading edge of the pulse is essentially governed by a maximal, constant population difference, $D \approx r$. This assumption linearizes Eq. (16) and permits direct solution of the set. The resulting intensity is a rising exponential:

$$I(t) = I_0 \exp[L(r-1)t/t_c \Delta L]. \quad (18)$$

The falling edge of the pulse may be characterized by a depleted gain, $D \approx 0$. With this approximation, Eq. (16) again becomes decoupled from Eq. (15) and may be solved to yield an exponentially decaying intensity:

$$I(t) \propto \exp(-Lt/t_c \Delta L). \quad (19)$$

One can crudely approximate the pulse width, t_p , by the sum of the rise time in Eq. (18) and the fall time in relation (19):

$$t_p = (rt_c \Delta L) / [L(r-1)]. \quad (20)$$

This equation represents a lower limit on t_p . Figure 5 compares the r dependence of t_p as predicted by Eq. (20) with the FWHM t_p given by Eqs. (1)–(5) for $\Delta L = 10 \mu\text{m}$ and $t_c = 10 \text{ nsec}$. In the large- r limit we see a reasonable, order-of-magnitude agreement between the two. This agreement, however, deteriorates quickly as r decreases, and the consequences of our approximations become evident.

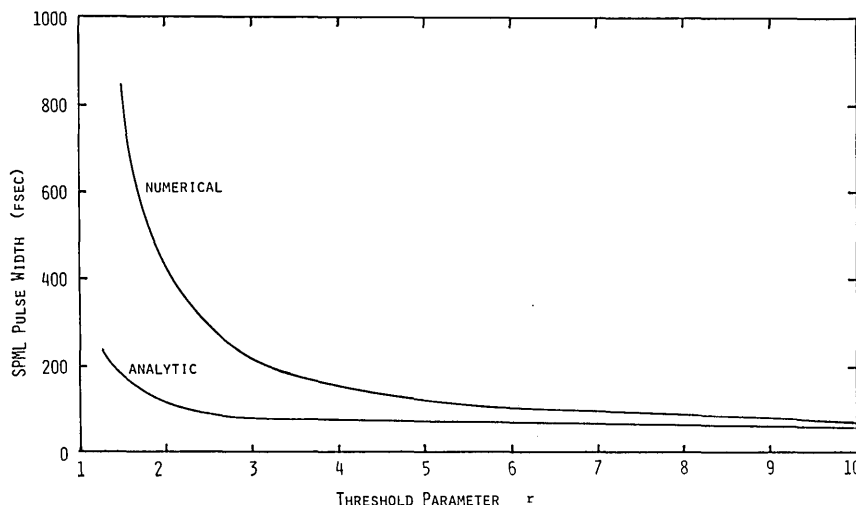


Fig. 5. Pulse width dependence on the threshold parameter, r , calculated using Eq. (20) and the set of Eqs. (1)–(5). In both cases, $\Delta L = 10 \mu\text{m}$ and $t_c = 10 \text{ nsec}$. There is qualitative agreement between the approximate analytic formula and the more exact numerical treatment.

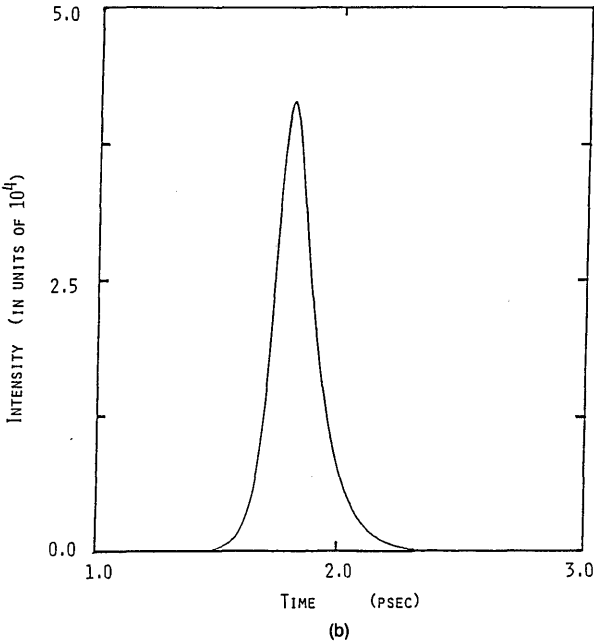
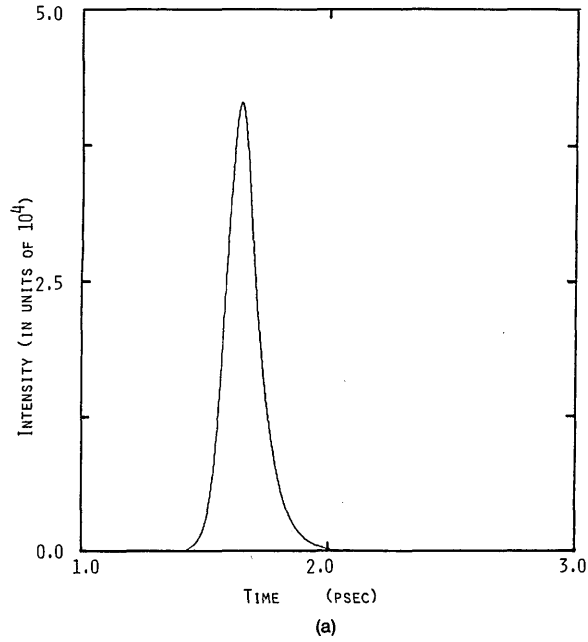


Fig. 6. (a) Typical SPML pulse numerically calculated from the Q-switching equations (15) and (16) for $\Delta L = 10 \mu\text{m}$ and $r = 3$. (b) Analytic fit suggested by Eq. (25).

In selecting an analytic pulse shape, one might consider numerically approximating Eqs. (15) and (16), by a curve-fitting technique, to the family of symmetric pulses,

$$I(t) = I_p \left\{ \text{sech} \left[rL(t - t_p) / (4nt_c \Delta L) \right] \right\}^n, \quad (21)$$

or the family of asymmetric pulses,

$$I(t) = I_p \left[1 + (t - t_p) / nt_0 \right]^n \exp \left[-(t - t_p) / t_0 \right], \quad (22)$$

for values of $t > t_p - nt_0$. A particular advantage of the pulses of the form of Eq. (22) is that one can calculate analytically their autocorrelation, which is the experimentally measured parameter. For example, the autocorrelation of Eq. (22) for $n = 1$ is

$$(|\tau| + 1) \exp(2 - |\tau|) \quad (23)$$

and for $n = 2$ is

$$(\tau^2 + 3|\tau| + 3) \exp(4 - |\tau|). \quad (24)$$

The normalized time, τ , in expressions (23) and (24) is in units of t_0 . In light of Eq. (18) and relation (19), however, one desires a pulse shape with an exponential rise and fall, and an example that satisfies these conditions is¹⁰

$$I(t) = I_{pk} r \exp \left[-L(t - T_{pk}) / (t_c \Delta L) \right] \times \left\{ \exp \left[-rL(t - T_{pk}) / (t_c \Delta L) \right] + r - 1 \right\}^{-1}. \quad (25)$$

Here, T_{pk} is the time at which the peak of the pulse occurs and may be calculated approximately from the initial (spontaneous-emission) intensity, I_0 , by

$$T_{pk} = (t_c \Delta L / L(1 - r)) \{ \ln [2I_0 t_c \Delta L (r - \ln r - 1) / \tau_2 L r] \}. \quad (26)$$

The numerical solution to the set Eqs. (15) and (16) is shown in Fig. 6(a), and Eq. (26) is shown in Fig. 6(b).

4. ZERO-DETUNING LIMIT

One might also consider Eqs. (12)–(14) in the limit of very small cavity detunings. If ΔL is allowed to go to zero, Eq. (14) implies $A = Q$, and we may adiabatically eliminate the electric field, A . This approximation is mathematically identical to considering a very short cavity lifetime, t_c , and hence is sometimes referred to as the bad-cavity limit in non-mode-locked lasers. This limit contrasts with the rate-equation limit in that this approximation retains the semiclassical effects. With this approximation our governing set of equations becomes

$$dD/dt = -(1/\tau_2)(2I), \quad (27)$$

$$dI/dt = -(2/T_s)(I - ID). \quad (28)$$

We have identified the intensity, I , with the square of the polarization, $I = A^2 = Q^2$. Noteworthy is that the population equation (27) is linear and hence is simpler than the population equation (15) of the rate-equation limit. An analytic solution to Eqs. (27) and (28) may be obtained subject to the initial conditions that $D(0^+) = r$, $I(0^+) = I_0$, where I_0 represents the spontaneous emission.

Dividing Eq. (27) by Eq. (28) and integrating gives the intensity as a function of the population difference:

$$I(D) = (\tau_2 / 2T_s) (-D^2 + 2D + r^2 - 2r + 2T_s I_0 / \tau_2). \quad (29)$$

Noting that the peak intensity again occurs at $D = 1$ allows us to write for I_{pk}

$$I_{pk} = (\tau_2 / 2T_s) [(r - 1)^2 + 2T_s I_0 / \tau_2]. \quad (30)$$

Equation (30) is plotted in Fig. 4 as a function of r for a negligible value of I_0 . We note that the quadratic form of Eq. (30) is more faithful to the exact theory of Eqs. (1)–(5) than its rate-equation counterpart.

Substituting Eq. (29) into Eq. (27) gives a nonlinear differential equation for D of the form

$$dD/dt = aD^2 + bD + c, \quad (31)$$

where

$$a = 1/T_s, \quad b = -2/T_s,$$

and

$$c = (-1/T_s)(r^2 - 2r + 2T_s I_0/\tau_2). \quad (32)$$

Equation (31) is a constantly forced Riccati equation that may be solved by making either the substitution

$$E(t) = [D(t) - \alpha]^{-1} \quad (33)$$

or the substitution

$$(T_s/F(t))dF/dt = [1 - D(t)] \quad (34)$$

or by direct integration, which is the method that we will illustrate. Separating Eq. (31) yields the integral,

$$\int_r^D (aD^2 + bD + c)^{-1} dD = t. \quad (35)$$

This integral is well tabulated,²⁶ and, pertinently, for $b^2 > 4ac$ the result is

$$t = (b^2 - 4ac)^{-1/2} \times \ln \frac{\{[2aD + b - (b^2 - 4ac)^{1/2}][2ar + b + (b^2 - 4ac)^{1/2}]\}}{\{[2aD + b + (b^2 - 4ac)^{1/2}][2ar + b - (b^2 - 4ac)^{1/2}]\}}. \quad (36)$$

Using Eqs. (30), (32), and (36), we may solve for the population difference, $D(t)$, explicitly:

$$D(t) = \frac{(1+k) - [r-1-k(r-k)](r-1+k)^{-1} \exp[(2k/T_s)t]}{1 - (r-1-k)(r-1+k)^{-1} \exp[(2k/T_s)t]}, \quad (37)$$

where

$$k = (2T_s I_{pk}/\tau_2)^{1/2}. \quad (38)$$

The time dependence of the population difference, $D(t)$, in Eq. (37) also describes the dynamics of the gain.

Substitution of Eq. (37) into Eq. (29) yields a closed expression for $I(t)$, which is plotted in Fig. 7 for our typical values of $r = 3$, $T_s = 50$ fsec, $\tau_2 = 5$ nsec, and the reasonable spontaneous emission level of 10^{-20} . The solution has a pulsed character of reasonable shape and energy when compared with Fig. 2. However, the pulse width predicted by Eq. (37) is approximately 44 fsec, a value that is considerably less than the 200-fsec figure calculated by using the more nearly complete model described by Eqs. (1)–(5). We note that this pulse width value of 44 fsec is essentially the value of the coherence time, $T_s = 50$ fsec. Conversely, the height is overstated by roughly a factor of 4. Further, the agreement is considerably worse than the rate-equation pulse of Fig. 6. Nonetheless, that the inherently semiclassical set of Eqs. (33) and (34) gives rise to reasonable pulses is an indication of the importance of semiclassical effects in SPML operation, particularly at small cavity length detunings.

If we ignore the effects of spontaneous emission, our solution for $I(t)$ may be written simply as

$$I(t) = [\tau_2(r-1)^2/2T_s] \text{sech}^2[(r-1)(t - T_{pk})/T_s]. \quad (39)$$

In Eq. (39), T_{pk} is the time when the peak of the output pulse occurs. From Eq. (36) with $D = 1$ and for small I_0 's, T_{pk} is

$$T_{pk} = [T_s/2(r-1)] \ln[8(r-1)^2 T_s I_0/\tau_2]. \quad (40)$$

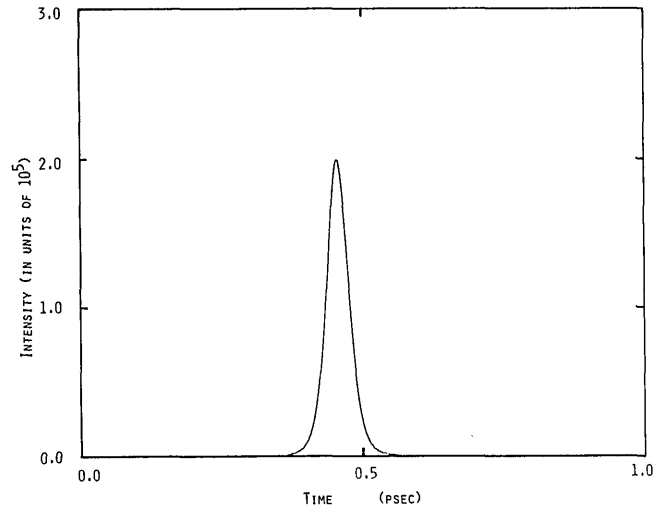


Fig. 7. Typical SPML pulse found from the analytic solution derived in the zero cavity detuning limit.

From Eq. (40) we see that T_{pk} is governed principally by T_s and I_0 . In our calculations we have assumed that the initial intensity is due to spontaneous emission. Equation (39) is an exact solution to our zero-detuning equations, a fact that may easily be verified by direct substitution into Eqs. (27) and (28). From Eq. (39) it follows that the FWHM pulse width in the zero-detuning limit is approximately

$$t_p = (1.7627)T_s/(r-1). \quad (41)$$

The hyperbolic secant form in Eq. (39) is a recurring one in the study of laser pulses. The popular formalism of Haus yields such a form for certain types of passively mode-locked laser,²⁷ and this result has been compared through experimental autocorrelation measurements with the output of a passively mode-locked dye laser.²⁸ A useful result given in Ref. 28 is the autocorrelation of a $\text{sech}^2(t/t_p)$ pulse:

$$G(\tau) = [\cosh(\tau/t_p) - (\tau/t_p)\sinh(\tau/t_p)]/\sinh^3(\tau/t_p). \quad (42)$$

We note, however, that our formalism is fundamentally distinct from that of Haus, and we believe that a better mathematical analogy may perhaps be drawn between ultrashort pulse production in zero-detuned SPML dye lasers and the phenomenon of self-induced transparency, which is governed by equations similar to Eqs. (27) and (28). Self-induced transparency was well studied by McCall and Hahn,²⁹⁻³¹ who also derived hyperbolic secant functions. Both in self-induced transparency and in our modeling of SPML dye lasers, one seeks steady-state pulse solutions to inherently semiclassical Maxwell-Schrödinger equations.

5. CONCLUSIONS

We have explored a nonlinear dynamical model of a SPML dye laser simplified principally by considering a delta-function pump. From a motivational standpoint, this is the regime where the newest SPML dye lasers operate.¹⁻³ Further approximations have led us to the interpretation that SPML dye lasers operated in the short-pump-pulse limit are predominantly gain-switched devices. Thus they can, in some sense, be described by the giant-pulse laser equations

derived in the early 1960's.⁶⁻⁹ We have also seen, however, that for quantitative agreement it is important to consider, among other things, semiclassical effects. Hence, in the laser system discussed in this paper, one is Q-switching a coherent laser medium.

More specifically, we have distilled our model into two simple sets, the rate-equation limit—Eqs. (15) and (16)—and the zero-detuning limit—Eqs. (27) and (28). The distinction between these two sets lies in the time constant of the intensity equation and in the degree of nonlinearity. Although they are slightly different, both of these sets qualitatively describe the ultrashort pulse production of SPML lasers. Further simplification of either set results in an absence of pulsed solutions. This leads us to identify the nonlinear term, ID , common to the intensity equation of both sets, as a critical mode-locking term. Physically, then, it is a saturating, nonadiabatically changing population difference that gives rise to SPML laser pulses. Not surprisingly, it is the large rate constant associated with the intensity equation that permits ultrashort pulse durations.

The delta-function limit is particularly important because, for a given dye and cavity, it defines the region of operation that gives the optimum, shortest output pulses. Furthermore, the ultrashort pump pulse provides degrees of freedom unique to synch-pumped systems; one does not have such optimization parameters in cw-pumped colliding-pulse mode-locked lasers.^{32,33} One might speculate that hybridly^{34,35} mode-locked laser systems driven by pulses of a few picoseconds could produce output pulses that compare favorably with those from current colliding-pulse mode-locked lasers.

ACKNOWLEDGMENT

This research was supported by the National Science Foundation. The authors have enjoyed the benefit of valuable discussions with Shuang Hua Jiang and Anthony A. Tovar.

REFERENCES

1. D. L. MacFarlane and L. W. Casperson, "Pump pulse effects in synchronously pumped mode-locked dye lasers," *J. Opt. Soc. Am. B* **6**, 292-299 (1989).
2. A. M. Johnson and W. M. Simpson, "Tunable femtosecond dye laser synchronously pumped by the compressed second harmonic of Nd:YAG," *J. Opt. Soc. Am. B* **2**, 619-625 (1985).
3. J. D. Kafka and T. Baer, "A synchronously pumped dye laser using ultrashort pump pulses," in *Ultrashort Pulse Spectroscopy and Applications* M. J. Soileau, ed., Proc. Soc. Photo-Opt. Instrum. Eng. **533**, 38-45 (1985); technical product information for Spectra-Physics Model 3800 mode-locked Nd:YAG laser, Model 3695 pulse compressor, and Model 3500 SPML dye laser (Spectra-Physics, Mountain View, Calif., 1988).
4. J. P. Heritage and R. K. Jain, "Subpicosecond pulses from a tunable cw mode-locked dye laser," *Appl. Phys. Lett.* **32**, 101-103 (1978).
5. L. W. Casperson, "Coherence effects in synchronously pumped mode-locked dye lasers," *J. Appl. Phys.* **54**, 2198-2208 (1983).
6. R. W. Hellwarth, "Theory of the pulsation of fluorescent light from ruby," *Phys. Rev. Lett.* **6**, 9-12 (1961).
7. A. A. Vuylsteke, "Theory of laser regeneration switching," *J. Appl. Phys.* **34**, 1615-1622 (1963).
8. W. G. Wagner and B. A. Lengyel, "Evolution of the giant pulse in a laser," *J. Appl. Phys.* **34**, 1615-1622 (1963).
9. C. C. Wang, "Optical giant pulses from a Q-switched laser," *Proc. IEEE* **51**, 1767 (1963).
10. L. W. Casperson, M. J. Herbst, and J. J. Turechek, "Pulse evolution in CO₂ lasers," *J. Appl. Phys.* **47**, 5099-5101 (1976).
11. D. Ricard and J. Ducuing, "Vibrational relaxation in the ground and first excited electronic states of large organic molecules in solution," *IEEE J. Quantum Electron.* **QE-10**, 745-746 (1974).
12. D. Ricard and J. Ducuing, "Vibrational relaxation in the ground electronic states of large organic molecules in solution," *J. Chem. Phys.* **62**, 3616-3619 (1975).
13. A. Penzkofer, W. Falkenstein, and W. Kaiser, "Vibronic relaxation in the S₁ state of rhodamine dye solutions," *Chem. Phys. Lett.* **44**, 82-87 (1976).
14. T. Yajima, H. Souma, and Y. Ishida, "Study of ultrafast relaxation processes by resonant Rayleigh-type optical mixing. II. Experiment on dye solutions," *Phys. Rev. A* **17**, 324-334 (1978).
15. M. M. Malley and G. Mourou, "The picosecond time-resolved fluorescence spectrum of rhodamine 6G," *Opt. Commun.* **10**, 323-326 (1974).
16. A. M. Weiner, S. DeSilvestri, and E. P. Ippen, "Three-pulse scattering for femtosecond dephasing studies: theory and experiment," *J. Opt. Soc. Am. B* **2**, 654-661 (1985).
17. B. K. Garside and T. K. Lim, "Ultrashort pulses from mode-locked cw dye lasers," *Opt. Commun.* **8**, 297-301 (1973).
18. B. K. Garside and T. K. Lim, "Passive mode-locking in flash-lamp-pumped dye lasers," *Opt. Commun.* **12**, 240-245 (1974).
19. Z. A. Yasa, "Theory of synchronously pumped dye lasers," *Appl. Phys. B* **30**, 135-142 (1983).
20. K. C. Reyzner and L. W. Casperson, "Polarization characteristics of dye-laser amplifiers II. Isotropic molecular distributions," *J. Appl. Phys.* **51**, 6083-6090 (1980).
21. E. N. Lorenz, "Deterministic non-periodic flows," *J. Atmos. Sci.* **20**, 130-141 (1960).
22. C. Sparrow, *The Lorenz Equations: Bifurcations, Chaos and Strange Attractors* (Springer-Verlag, Berlin, 1982).
23. H. Haken, "Analogy between higher instabilities in fluids and lasers," *Phys. Lett.* **53A**, 77-78 (1975).
24. P. W. Milonni, R. B. Gibson, and A. J. Taylor, "Ultrashort pulse propagation in KrF laser amplifiers," *J. Opt. Soc. Am. B* **5**, 1360-1368 (1988).
25. J. M. Catherall, G. H. C. New, and P. M. Radmore, "Approach to mode locking by synchronous pumping," *Opt. Lett.* **7**, 319-321 (1982).
26. H. B. Dwight, *Tables of Integrals and Other Mathematical Data* (Macmillan, New York, 1961), p. 38, 160.01.
27. H. A. Haus, "Theory of mode locking with a slow saturable absorber," *IEEE J. Quantum Electron.* **QE-11**, 736-746 (1975).
28. H. A. Haus, C. V. Shank, and E. P. Ippen, "Shape of passively mode-locked laser pulses," *Opt. Commun.* **15**, 29-31 (1975).
29. S. L. McCall and E. L. Hahn, "Self-induced transparency by coherent light," *Phys. Rev. Lett.* **18**, 908-911 (1967).
30. S. L. McCall and E. L. Hahn, "Self-induced transparency," *Phys. Rev.* **183**, 457-485 (1969).
31. S. L. McCall and E. L. Hahn, "Pulse-area-pulse-energy description of a traveling-wave laser amplifier," *Phys. Rev. A* **2**, 861-870 (1970).
32. R. L. Fork, B. I. Greene, and C. V. Shank, "Generation of optical pulses shorter than 0.1 psec by colliding pulse mode-locking," *Appl. Phys. Lett.* **38**, 671-672 (1981).
33. W. Dietal, "Transient absorber gratings shorten the pulses of a passively mode-locked cw dye laser," *Opt. Commun.* **43**, 69-71 (1982).
34. G. W. Fehrenbach, K. J. Gruntz, and R. G. Ulbrich, "Subpicosecond light pulses from a synchronously mode-locked dye laser with composite gain and absorber medium," *Appl. Phys. Lett.* **33**, 159-160 (1978).
35. G. A. Mourou and T. Sizer II, "Generation of pulses shorter than 70 fs with a synchronously-pumped cw dye laser," *Opt. Commun.* **41**, 47-48 (1982).